Research article

Selen Postaci, Bilge Can Yildiz, Alpan Bek and Mehmet Emre Tasgin*

Silent enhancement of SERS signal without increasing hot spot intensities

https://doi.org/10.1515/nanoph-2018-0089
Received July 6, 2018; revised September 2, 2018; accepted September 10, 2018

Abstract: Plasmonic nanostructures enhance nonlinear response, such as surface enhanced Raman scattering (SERS), by localizing the incident field into hot spots. The localized hot spot field can be enhanced even further when linear Fano resonances take place in a double resonance scheme. However, hot spot enhancement is limited with the modification of the vibrational modes, the breakdown of the molecule, and the tunneling regime. Here, we present a method which can circumvent these limitations. Our analytical model and solutions of 3D Maxwell equations show that: enhancement due to the localized field can be multiplied by a factor of 10^2–10^3. Moreover, this can be performed without increasing the hot spot intensity which also avoids the modification of the Raman modes. Unlike linear Fano resonances, here, we create a path interference in the nonlinear response. We demonstrate on a single equation that enhancement takes place due to cancellation of the contributing terms in the denominator of the SERS response. Our method can be implemented on an atomic force microscope tip, decorated (or "contaminated") with appropriate quantum emitters.

Keywords: Fano resonance; surface enhanced Raman scattering; hot spot; nonlinear plasmonics; plasmon modes.

***Corresponding author: Mehmet Emre Tasgin,** Institute of Nuclear Sciences, Hacettepe University, Ankara 06800, Turkey, e-mail: metasgin@hacettepe.edu.tr.
http://orcid.org/0000-0001-8483-6881
Selen Postaci: Institute of Nuclear Sciences, Hacettepe University, Ankara 06800, Turkey; and Department of Physics, Middle East Technical University, Ankara 06800, Turkey
Bilge Can Yildiz: Department of Applied Physics, Atilim University, Ankara 06836, Turkey
Alpan Bek: Department of Physics, Middle East Technical University, Ankara 06800, Turkey; The Center for Solar Energy Research and Applications (GUNAM), Middle East Technical University, Ankara 06800, Turkey; and Micro and Nanotechnology Program of Graduate School of Natural and Applied Sciences, Middle East Technical University, Ankara 06800, Turkey

1 Introduction

When metal nanoparticles (MNPs) interact with light, surface plasmons are induced in the form of collective oscillations in electrons. The regions where the incident electromagnetic field is confined and highly enhanced are called the hot spots [1, 2]. Field intensity at the hot spots can be 5 orders of magnitude larger compared to the incident one [3]. It is also reported that self-repeating cascaded materials can confine light even better compared to the gaps between MNPs [4, 5]. Intense fields give rise to appearance of nonlinear processes such as second harmonic generation (SHG), four wave mixing (FWM), and surface enhanced Raman scattering (SERS) [1, 6, 7]. A nonlinear process becomes stronger when the input (driving) and the converted frequencies match with two plasmon resonances, i.e. double resonance scheme [8].

Hot spots also provide enhanced light-matter interaction. When a quantum emitter (QE) is placed in a hot spot, the localized plasmon field interacts strongly with the QE. A small decay rate of the QE creates Fano resonances, a dip in the plasmonic spectrum [9, 10]. In this process, the localized plasmon field provides a weak hybridization. Fano resonance also appears when excited plasmon mode couples to a long-life dark plasmon mode [9–14]. Fano resonances are also shown to provide control over other nonlinear processes such as SHG [15, 16], third harmonic generation [17], and FWM [18, 19].

Fano resonances can extend the lifetime of plasmon excitations [20–23] which makes the operation of coherent plasmon emission (spaser) possible [24]. They also lead to further enhancement of the localized hot spot field [25]. This extra enhancement in the hot spot field is cleverly adapted for the enhancement of the nonlinear response in FWM [26] and SERS [5, 27, 28]. Similar to a double resonance scheme [8], both the excited and Stokes shifted frequencies are aligned with two Fano resonances [5, 27, 28]. The double Fano resonance scheme provides much stronger enhancement in the SERS signal.

SERS is a very useful chemical analysis technique. It provides information about the chemical composition of newly synthesized molecules by determining the existing

bond types. Single-molecule detection via SERS is used in many fields of science, including chemistry [29], nanobiology [30], tumor targeting, and cancer applications [31]. Even more, mapping of inner structure and surface configuration of a single molecule is achieved recently [29] using a double resonance scheme [8]. Such an imaging requires very intense fields at the nanometer-size hot spots. When the imaging tip gets closer to the metal surface, the intensity at the hot spot – where the molecule lies – increases. If the hot spot intensity is increased further, e.g. in a double Fano resonance scheme [5, 27, 28], fragile molecules can be damaged [32, 33]. It is also experimented that vibrational modes of a Raman-imaged nanostructure (e.g. a carbon nanotube) can be modified due to the close spacing of the tip [34]. Additionally, electron tunnelling can limit the intensity enhancement in the gaps [35].

In this manuscript, we study the SERS signal from a double resonance system. A Raman reporter molecule is placed close to the gap of a MNP dimer (see Figure 1). We additionally place an auxiliary QE (e.g. a molecule or a nitrogen vacancy center) to the other side of the gap. We present a "proof of principal" demonstration of the following phenomenon. It is possible to enhance the SERS signal without enhancing the hot spot intensities. Exact solutions of 3D Maxwell equations show that SERS signal can be enhanced by a factor of 10^2–10^3 without increasing the field intensities at the excited and the Stokes-shifted hot spots. This enhancement multiplies the enhancement due to localization. That is, localization of both fields, the excited and the Stokes-shifted, already enhances the Raman signal by a factor of, e.g. 10^8 [8]. Our method raises the enhancement to 10^{10}–10^{11} in this case. In this work, we not only perform 3D simulations but also explicitly demonstrate the underlying physics within a basic analytical model.

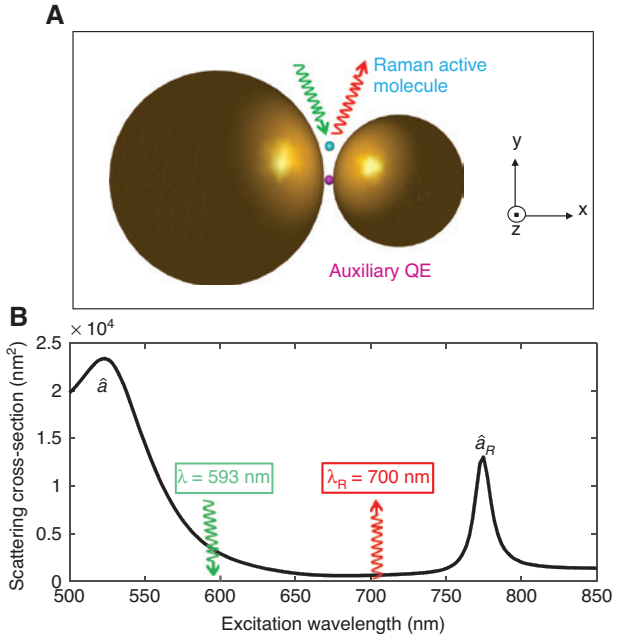

Figure 1: Enhancement of SERS signal with the help of an auxiliary QE. (A) The setup we consider for a double resonance scheme. A gold MNP dimer manifests two plasmon modes, depicted in (B). A Raman-active molecule (blue), placed close to the dimer gap, produces the Stokes signal. A QE (purple) is positioned in the vicinity of the gap and interacts with the $\hat{a}_R$ plasmon mode, into which the Stokes signal emerges. (Details can be found in the text.) The presence of the QE does not change the intensity on the Raman-active molecule but enhances the Stokes signal.

The presented phenomenon can be adapted to further increase the efficiency of SERS imaging for systems that are already operating in the breakdown or tunneling regimes. This can be vital in the SERS imaging of small Raman-response materials. In addition, better signal intensities with larger tip-surface spacing, or with smaller laser intensities, can be achieved which can avoid modifications in the Raman vibrational modes.

The manuscript is organized as follows. We first introduce our setup for a double plasmon resonance system in Section 2. Next, in Section 3, we present a basic analytical model. In this model, we show that presence of an aux QE can enhance (Section. 3.2) or suppress (Section 3.3) the Raman process. In Section 4, we perform SERS simulations with the exact solutions of the 3D Maxwell equations. We test the retardation effects. We observe that the anticipated enhancement is present. Section 5 contains a summary and our brief discussions.

2 Setup

In an efficient conversion, nonlinear process takes place between plasmonic excitations of different frequencies due to the localization [8, 36, 37]. Recent studies show that MNPs with plasmon resonances at both excitation and Stokes frequencies (double resonance) provide better enhancement factors for Raman intensities [8, 38, 39]. For this reason, we study a double resonance system in this work.

We consider a gold MNP dimer (see Figure 1A). The two MNPs, of diameters 90 nm and 55 nm, are separated by a gap of 4 nm. The dimer is illuminated with an x-polarized plane-wave source propagating along the y-direction. The scattering cross-section of the the dimer, Figure 1B, manifests two plasmon modes, $\hat{a}$ and $\hat{a}_R$, with resonances $\Lambda = c/\Omega = 530$ nm and $\Lambda_R = c/\Omega_R = 780$ nm, respectively. Electric field profiles of the two resonances (hot spots) are depicted in Figure 2A and B. In obtaining Figures 1B and 2 we use the experimental, frequency dependent,

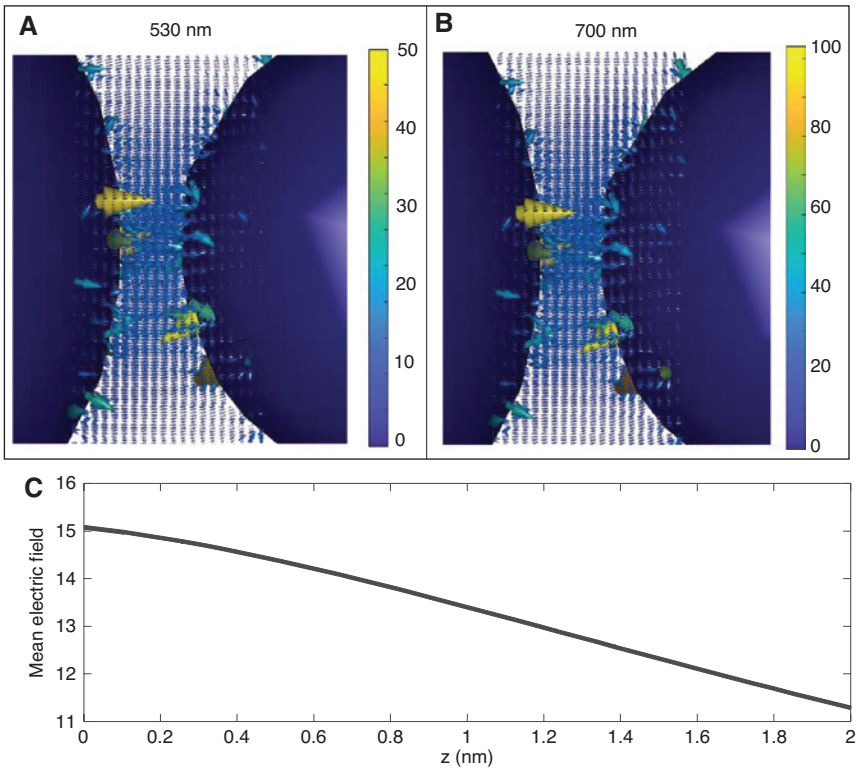

Figure 2: Hot spots where Raman conversion and its enhancement take place.
(A, B) Electric field profiles of the two plasmon modes given in Figure 1B. Hot spots of the two modes overlap. (C) Mean electric field on the QE, which is proportional with the overlap integral [40] f, versus the position of the QE. (In units of incident electric field.)

dielectric function for gold. We perform the simulations with MNPBEM [41], a freeware Maxwell solver based on boundary elements method.

A strong incident laser field, $\lambda_L = c/\omega = 593$ nm, excites the plasmons in the $\hat{a}$ mode. We position a Raman-active molecule (blue in Figure 1A) of diameter 4 nm [42] close to the two hot spots. The substantial overlap between the hot spots of the two modes, $\hat{a}$ and $\hat{a}_R$, and the Raman reporter molecule yields a significant overlap integral χ for the Stokes Raman process. Hence, a plasmon in the excited $\hat{a}$ mode generates a Stokes shifted plasmon with $c/\omega_R = \lambda_R = 700$ nm in the lower energy mode[1] $\hat{a}_R$ [8, 38, 39]. We consider a single vibrational mode, $\nu = 2600$ cm^{-1} [45], for the Raman reporter molecule for simplicity and in order to gain a basic understanding on the path interference effects.

When an auxiliary QE is inserted in the system, purple in Figure 1A, it also interacts strongly with the hot spot of the $\hat{a}_R$ mode, into which the nonlinear conversion takes place. Level spacing of the QE, ω_{eg}, is chosen about Ω_R. As will be apparent in the following discussions, $\lambda_{eg} = c/\omega_{eg}$ is chosen to be off-resonant to both plasmon resonances, e.g. ~830 nm. By moving the QE along the z axis, we tune the coupling (designated as f in Section 3.1) between the QE and the $\hat{a}_R$ mode. The diameter of the QE is set to 2 nm. In the analytical model it is treated as a two-level system. In the 3D simulations, in Section 4, QE is modeled by a Lorentzian dielectric function [3] of decay rate $\gamma_{eg} \simeq 2 \times 10^{11}$ Hz. This corresponds to a low-quality QE. That is, it is much larger than the typical values of ~10^9 Hz.

3 A basic analytical model

In the following, we present a basic analytical model from which we anticipate the presence of the enhancement. We study the setup in Figure 1. We introduce the effective Hamiltonian for a double resonance SERS system coupled

1 Involvement of plasmons in a frequency conversion process [36] increases the overlap integral [40, 43] several orders of magnitude because both the excited and the converted modes are strongly localized compared to the incident plane waves [8]. In the far field, one observes the damping of the plasmon due to radiation reaction or recombination of the pairs into which plasmon decays [44]. Far-field Raman signal is proportional to the number of Stokes-shifted plasmons.

with an auxiliary QE. We get the equations of motion (EOM) using Heisenberg equations. We obtain a simple expression for the steady state of the Stokes field amplitude, Eq. (12). On this expression we explain why the pronounced enhancement should emerge.

3.1 Hamiltonian equation and equations of motion

Hamiltonians for such a system, including the Raman conversion, can be written as the sum of the terms $\hat{H}_0+\hat{H}_{QE}+\hat{H}_L+\hat{H}_{int}+\hat{H}_R$, with

$$\begin{aligned}\hat{H}_0&=\hbar\Omega\hat{a}^\dagger\hat{a}+\hbar\Omega_R\hat{a}_R^\dagger\hat{a}_R+\hbar\Omega_{ph}\hat{a}_{ph}^\dagger\hat{a}_{ph}\\ \hat{H}_{QE}&=\hbar\omega_{eg}|e\rangle\langle e|\\ \hat{H}_L&=i\hbar(\hat{a}^\dagger\varepsilon e^{-i\omega t}-\hat{a}\varepsilon^* e^{i\omega t}),\\ \hat{H}_{int}&=\hbar(f\hat{a}_R|e\rangle\langle g|+f^*\hat{a}_R^\dagger|g\rangle\langle e|),\\ \hat{H}_R&=\hbar\chi(\hat{a}_R^\dagger\hat{a}_{ph}^\dagger\hat{a}+\hat{a}^\dagger\hat{a}_{ph}\hat{a}_R),\end{aligned}\tag{1}$$

where $\hat{H}_0$ includes the energies for the driven $\hat{a}$, and Raman shifted $\hat{a}_R$ plasmon modes as well as the molecular vibrations, $\hat{a}_{ph}$. $\hat{H}_{QE}$ is the energy of the auxiliary QE, which is considered to be a two-level state with ground and excited levels. The ground state energy is taken to be 0 for simplicity [46]. $\hat{H}_L$ is the driving of the laser pump, $\hat{H}_R$ denotes the Raman process, and $\hat{H}_{int}$ is the interaction of the Stokes-shifted plasmon polaritons of $\hat{a}_R$ mode with the auxiliary QE. χ determines the strength of the Raman process, while ε is proportional to the amplitude of the incident laser source. Here, we do not consider the anti-Stokes shift in the Hamiltonian to simplify our results, however, we have verified that the enhancement values and the spectroscopic behavior of the system remain similar in such a case. The couplimg strength between the auxiliary QE and $\hat{a}_R$ mode is denoted by f [40]. Coupling of the auxiliary QE to $\hat{a}$ mode is not considered due to far-off resonance and simplicity. $|g\rangle$ and $|e\rangle$ represents the ground and excited states for the auxiliary QE. $\hat{H}_R$ is a standard Hamiltonian for a Raman process, described, for instance, in Refs. [8, 38, 39]. (A similar form of $\hat{H}_R$ could have also been derived in the Supplementary Material [47] from a radiation pressure like interaction [48, 49]). We obtain the dynamics via Heisenberg equations, $i\hbar\dot{\hat{a}}=[\hat{a},\hat{H}]$. We note that, since we do not consider the quantum optical effects, we are able to replace the operators with complex numbers [50]; $\hat{a}\to\alpha$, $\hat{a}_R\to\alpha_R$, $\hat{a}_{ph}\to\alpha_{ph}$, $\hat{\rho}_{eg}=|e\rangle\langle g|\to\rho_{eg}$. We find the EOM as

$$\dot{\alpha}_R=(-i\Omega_R-\gamma_R)\alpha_R-i\chi\alpha_{ph}^*\alpha-if^*\rho_{ge},\tag{2}$$

$$\dot{\alpha}=(-i\Omega-\gamma)\alpha-i\chi\alpha_{ph}\alpha_R+\varepsilon e^{-i\omega t},\tag{3}$$

$$\dot{\alpha}_{ph}=(-i\Omega_{ph}-\gamma_{ph})\alpha_{ph}-i\chi\alpha_R^*\alpha+\varepsilon_{ph}e^{-i\omega_{ph}t},\tag{4}$$

$$\dot{\rho}_{eg}=(-i\omega_{eg}-\gamma_{eg})\rho_{eg}+if\alpha_R(\rho_{ee}-\rho_{gg}),\tag{5}$$

$$\dot{\rho}_{ee}=-\gamma_{ee}\rho_{ee}+if^*\alpha_R^*\rho_{eg}-if\alpha_R\rho_{eg}^*,\tag{6}$$

where we introduce the damping rates γ, γ_R, γ_{ph}, γ_{eg}, and γ_{ee} [46, 50]. We also have the constraint $\rho_{ee}+\rho_{gg}=1$. ε_{ph} is introduced for the vibrations, due to the finite ambient temperature [48, 49]. Its actual value has no influence on the relative enhancement/suppression factors.

In the steady state, solutions are in the form $\alpha_R(t)=\tilde{\alpha}_R e^{-i\omega_R t}$, $\alpha(t)=\tilde{\alpha}e^{-i\omega t}$, $\alpha_{ph}(t)=\tilde{\alpha}_{ph}e^{-i\omega_{ph}t}$, $\rho_{eg}(t)=\tilde{\rho}_{eg}e^{-i\omega_R t}$, $\rho_{ee}(t)=\tilde{\rho}_{ee}$, where exponentials cancel in each equation, Eqs. (2)–(6). In other words, this is the energy conservation in the long-term limit. Eqs. (2)–(6) become

$$[i(\Omega_R-\omega_R)+\gamma_R]\tilde{\alpha}_R=-i\chi\tilde{\alpha}_{ph}^*\tilde{\alpha}-if^*\tilde{\rho}_{eg},\tag{7}$$

$$[i(\Omega-\omega)+\gamma]\tilde{\alpha}=-i\chi\tilde{\alpha}_{ph}\tilde{\alpha}_R+\varepsilon,\tag{8}$$

$$[i(\Omega_{ph}-\omega_{ph})+\gamma_{ph}]\tilde{\alpha}_{ph}=-i\chi\tilde{\alpha}_R^*\tilde{\alpha}+\varepsilon_{ph},\tag{9}$$

$$[i(\omega_{eg}-\omega_R)+\gamma_{eg}]\tilde{\rho}_{eg}=if\tilde{\alpha}_R(\tilde{\rho}_{ee}-\tilde{\rho}_{gg}),\tag{10}$$

$$\gamma_{ee}\tilde{\rho}_{ee}=-if\tilde{\alpha}_R\tilde{\rho}_{eg}^*+if^*\tilde{\alpha}_R^*\tilde{\rho}_{eg}.\tag{11}$$

we can obtain a simple expression for the Stokes-shifted plasmon amplitude (SERS signal) by using Eqs. (7) and (9)

$$\tilde{\alpha}_R=\frac{-i\chi\varepsilon_{ph}^*}{\beta_{ph}^*\left([i(\Omega_R-\omega_R)+\gamma_R]-\dfrac{|f|^2y}{[i(\omega_{eg}-\omega_R)+\gamma_{eg}]}\right)-|\chi|^2|\tilde{\alpha}|^2}\tilde{\alpha},\tag{12}$$

where $\beta_{ph}=[i(\Omega_{ph}-\omega_{ph})+\gamma_{ph}]$. Here $y=\rho_{ee}-\rho_{gg}$ is the population inversion for the auxiliary QE. $|\chi|^2|\tilde{\alpha}|^2$ term is small compared to the others in the denominator and, hence, can be neglected.

We use Eq. (12) merely to anticipate the enhancement/suppression effects. All the presented results are obtained by numerical time evolution of Eqs. (2)–(6), with the initial conditions $\alpha(t=0)=\alpha_R(0)=0$ and $\rho_{ee}(t=0)=\rho_{eg}(0)=0$.

3.2 Enhancement

A quick examination of the denominator of Eq. (12) reveals that for the proper choice of ω_{eg}, nonresonant term $(\Omega_R - \omega_R)$ in the denominator can be canceled with the term containing f, the MNP-QE coupling. The condition is

$$\omega_{eg}^{*} = \omega_R + \frac{|f|^2 y}{2(\Omega_R - \omega_R)} - \sqrt{\frac{|f|^4 |y|^2}{4(\Omega_R - \omega_R)^2} - \gamma_{eg}^2}. \tag{13}$$

This choice for the level spacing enables us to minimize the denominator, consequently enhancing the Raman signal amplitude.

To examine the dependence of the enhancement with respect to the level spacing ($\lambda_{eg} = c/\omega_{eg}$), we time evolve the EOM (2)–(6) where initially QE is in the ground state and occupations of the plasmon modes are 0. The parameters are chosen as $\gamma = 0.01\omega$, $\gamma_R = 0.005\omega$, and $\gamma_{ph} = 0.001\omega$. Nevertheless, one can realize that Ω_{ph} and γ_{ph} play no role in the cancellation of the denominator in Eq. (12). The damping rate (spectral width) of the auxiliary QE is taken to be $\gamma_{eg} = 10^{-5}\omega$. Here, the frequency of the incident light (ω) is related to λ_L as $\omega = c/\lambda_L = 593$ nm. χ is assumed a small value $10^{-5}\omega$, where it is verified that the value of χ does not affect the enhancement factors, and we take $\varepsilon = 0.1\omega$. f is also varied in order to explore the effect of the coupling in the MNP-QE system. The enhancement factor is calculated with respect to the $|\alpha_R|^2$ intensity for $f = 0$.

The results are depicted in Figure 3A, where enhancement factors of ≈300 are observed. As suggested by Eq. (13), $\Omega_R < \omega_R$, cancellation (enhancement) takes place for longer wavelengths as MNP-QE coupling, f, increases. The spectral position of $\lambda_{eg}^{*} = c/\omega_{eg}^{*}$ also justifies our assumption for off-resonant $\hat{a}$-QE coupling. If Eq. (12) is examined, it can be realized that the amount of enhancement can be increased by introducing more interference paths via additional QEs [18] or additional plasmon conversion modes.

Equation (12) is a single and simple equation that enables us to predict possible interference effects without including the complications emerging in 3D simulations. Before moving forward, we underline that our aim is to present a simple understanding for the enhancement process, without getting lost in details.

Linear Fano resonances, dark-hot resonances [25] which enhance the hot spot intensity, appear if one of the two coupled oscillators has longer lifetime [9, 12, 13, 51]. Here, interference of the nonlinear frequency conversion paths demonstrates to us an interesting incident. Even when the spectral width (damping rate) of the auxiliary object is equal to the damping rate of the MNP hot spot, 25 times enhancement can emerge due to cancellation in the denominator of Eq. (12). The presented enhancement factor is obtained for a plasmon mode of fair quality $\gamma = 0.01\omega$. When an MNP with higher quality factor plasmon resonance [52–55] is used, available enhancement factor grows up.

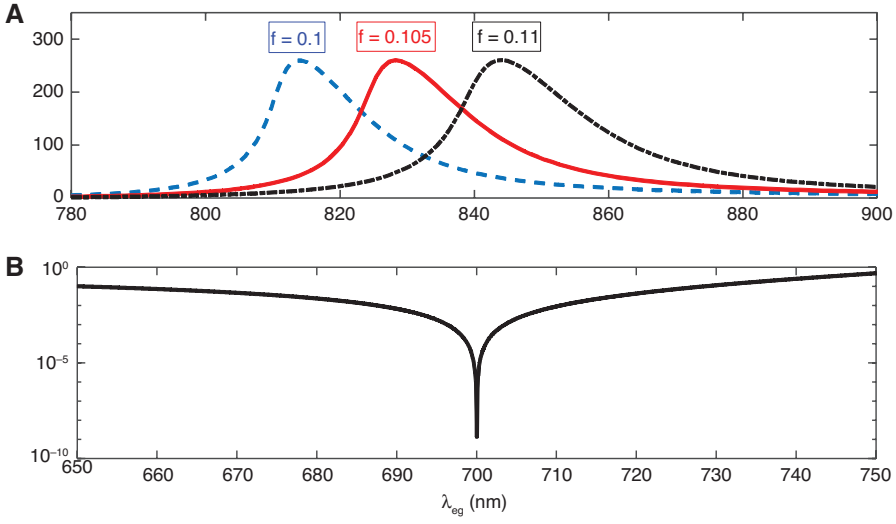

Figure 3: Analytical results.
(A) Enhancement and (B) suppression of the SERS signal due to path interference effects. Presence of an aux QE, of level spacing $\omega_{eg} = c/\lambda_{eg}$, can lead to (A) cancellation or (B) growth in the denominator of the SERS response, in Eq. (12).

3.3 Suppression

Our model also predicts that SERS can be suppressed several orders of magnitude (Figure 3B) for the choice of the auxiliary QE as $\omega_{eg}=\omega_R$. Simply, for this case, Fano resonance (transparency) prohibits the plasmon oscillations of the converted frequency ω_R from emerging into the $\hat{a}_R$ mode. One can realize that path interference in the nonlinear response is actually not so different from the one taking place in the linear response [51]. That is, the modification of the denominator in both the nonlinear [18, 37] and the linear responses [21] have a common form [43].

A similar silencing phenomenon is observed in the SHG experiments and in 3D simulations [56] and can be demonstrated with a simple analytical model [37]. The denominator of Eq. (12) also shows why a suppression effect can take place similar to the one observed in SHG [56]. If one chooses $\omega_{eg}=\omega_R$, the extra term becomes $\gamma_{eg}^{-1}|f|^2 y$. This term is very large since $\gamma_{eg}^{-1}\sim 10^5$ and $f=0.1$ in units scaled with the laser frequency ω (≈PHz). We stress that Figure 3 is generated through the exact time evolution of Eqs. (2)–(6). That is, no approximation is used to obtain the results.

4 Three-dimensional simulations

We also perform simulations with the exact solutions of 3D Maxwell equations and use the setup in Figure 1. We note in advance that we do not aim a one-to-one comparison between the analytical solutions and the 3D simulations. We neither aim to provide a setup which we claim to work perfectly in an experiment. Here, we aim to observe if the retardation effects wipe out the enhancement phenomenon predicted by our basic analytical model, or not. Making a one-to-one comparison between the theoretical findings and the 3D simulations, which is a very sophisticated process, is out of the scope of this work.

In the electromagnetic simulations, we use the setup in Figure 1A described in Section 2 in detail. We examine if the presence of the aux QE, which we model by a Lorentzian dielectric function $\varepsilon(\omega)$ [3], modifies the SERS intensity. In the absence of an appropriately chosen QE, SERS enhancement due to localization can be calculated by multiplying the enhancements of the two fields, exciting (593 nm) and Stokes-shifted (700 nm) fields, i.e. $EF(\omega)\times EF(\omega_R)$ [27]. This is the enhancement due to localization (SERS) already present in the system. This enhancement can be as high as 10^8 [8]. However, the extra enhancement via path interference cannot be modeled with the same method [27]. For the path interference, we use the method [57] in the freeware program MNPBEM [41].

We show that an extra enhancement (Figure 4) appears when the QE is present. We check that in the presence of the QE, profiles of the two *fields* (593 nm and 700 nm) *do not change* on the Raman-active molecule compared to Figure 2. In other words, extra (interference) enhancement appears without exposing the Raman-active molecule to stronger fields and thereby heating it to its breakdown.

In Figure 4, we observe that the extra enhancement is positioned (λ_{eg}^*) on the correct (right hand) side of the $\hat{a}_R$ mode as predicted by Eq. (13). That is, λ_{eg} must be on the longer wavelengths to perform a cancellation in the denominator of Eq. (12). In Figure 4, we also change the position of the auxiliary QE along the z axis in order to alter the interaction with the MNP. When distance to the hot spot center (z), increases, the interaction of the plasmon mode with the auxiliary QE (Figure 2C) decreases. We observe that enhancement occurs at larger wavelengths for stronger MNP-QE coupling as suggested by the basic model in Figure 3. Furthermore, maximum enhancement in Raman signal takes place around $\lambda_{eg}^*\simeq 834$ nm, which is farther apart from the Stokes line $\lambda_R=700$ nm. A linear Fano resonance would yield the strongest hot spot enhancement when $\lambda_{eg}\simeq\lambda_R$ [25]. λ_{eg}^* is taken to be far from the Stokes line both in our simple model and in 3D simulations. However, stronger interaction f does not always enhance SERS. When auxiliary QE is positioned much closer to the dimer center, we observe that enhancement decreases 2 orders of magnitude, see Supplementary Material [47]. This is also observed in SHG process [15].

Even though many complications may arise in 3D solutions the results match "qualitatively" with our basic model as a "proof of principal" demonstration. Our

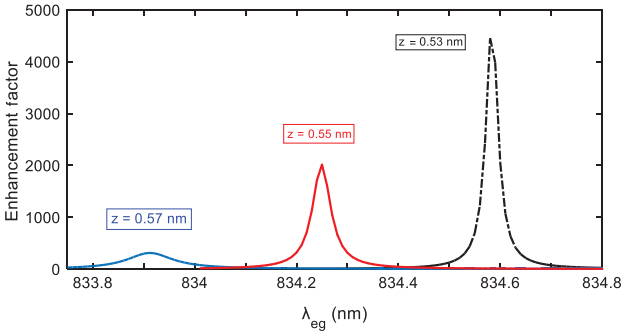

Figure 4: Exact solutions of the 3D Maxwell equations. Extra enhancement of SERS via path interference phenomenon. Presence of a QE, in Figure 1A, does not change the localization of the fields on the Raman-active molecule (localization enhancement remains unchanged). The presented enhancement factors, up to 5000, multiply the localization enhancement. The extra (interference) enhancement appears in the spectral position predicted by the analytical model, in Eq. (13), and shifts to longer wavelengths with stronger QE coupling (Figure 3A).

analytical model does not take into account (i) the change in the density of states, i.e. Purcell effect, (ii) coupling of the fields to possible dark modes, and (iii) the retardation effects. In Figure 4, retardation effects allow Fano resonances to appear in a narrower band compared to our model, similar to Ref. [37].

It can be seen even in the simple setting of Figure 1, a setting which can be optimized by further elaboration, that there is an average of a factor of 10^2–10^3 further enhancement factor is achieved at a QE distance of ±1 nm from the MNPs. One can realize that the hot spot field intensity within the 4 nm gap between MNPs is not a particularly strong one compared to the nanostructures where hot spot is enhanced 10^5–10^6 times. Also, there are structures, for instance, a metal-coated atomic force microscope (AFM) tip, which possess a wider hot spot. In such kind of setups, similar order of enhancement as in Figure 2 can be achieved without accurate positioning of the QE(s).

Our problem setting, which involves configuration of a MNP dimer coupled to a Raman reporter molecule and an auxiliary QE, can be implemented controllably using several nanotechnological methods such as e-beam lithography [58, 59] or DNA based biomolecular recognition [60, 61] that provide ultimate nanoscale spatial control, see Supplementary Material [47]. One can also conduct an experiment based on the stochastic distributions of many molecules [15].

A practical implementation (Figure 5) could be described as follows. A gold-coated AFM tip localizes the incident radiation into the tip apex in the form of plasmon excitations. The strong localized field results in tip enhanced Raman scattering (TERS) when there is a Raman-active molecule (blue in Figure 5) on a substrate. Ref. [62], as an example, demonstrates that such a tip supports three plasmon modes in the optical regime. When the middle (second) plasmon mode is excited, Stokes shifted Raman signal takes place into the longer wavelength (third) plasmon mode. Hence, these two modes can be used as a double resonance SERS (TERS) system. When the AFM tip is decorated (can also be considered as contamination) with carefully chosen molecules (QEs), purple in Figure 5, it will produce more intense TERS signal without increasing near-field intensity. Decoration of the tip edge with QEs can be performed using a technique reminiscent of dip-pen lithography. We already know that in spasers [24], where MNPs are surrounded by molecules, linear Fano resonance increases the plasmon lifetime and fluorescence intensity of the molecules [4]. Fano resonances can also be adapted in an all-plasmonic setting [63, 64].

Unlike the enhancement effect, the suppression phenomenon – neither in the SHG [37] nor in the Raman cases – cannot be demonstrated with the 3D simulations of Ref. [57]. This is simply because 3D simulation method [57] is only a first-order approach. Demonstration of the suppression phenomenon necessitates the self-consistent solution of Maxwell equations, as in Eqs. (2)–(6). Self-consistent 3D simulation of a Raman process is a numerical art on its own.

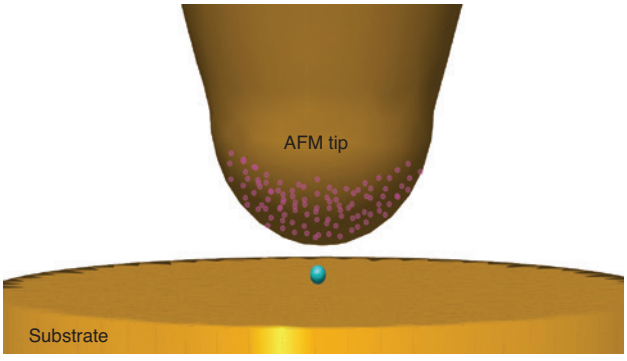

Figure 5: A practical implementation of the extra enhancement. A gold-coated AFM tip can support more than one plasmon resonance [62], similar to Figure 1B. A strong field, localized at the edge of the tip, interacts with a Raman-active molecule (blue) and leads to an enhanced Raman signal. When the tip is decorated (it can as well be called "contaminated") with auxiliary QEs (purple), of level spacing not close to either the exciting or the Stokes-shifted frequencies, the localized field on the Raman-active molecule remains unchanged. Still, QEs give rise to extra enhancement of the Raman signal from Raman-active molecule(s) due to Fano (interference) effect.

5 Summary and discussions

We introduce a new method which can increase the SERS signal without increasing the hot spot intensities. In other words, SERS signal can be multiplied by a factor of 10^2–10^3, on top of the hot spot formation by plasmon mediated field enhancement, without heating the Raman reporter molecule any further. This is different than linear Fano resonances which enhance the hot spot field [5, 27, 28]. The phenomenon takes place due to the modification of the Raman conversion paths, in the presence of an auxiliary QE or a dark mode, see Supplementary Material [47]. Both the 10^2–10^3 enhancement and the unvarying hot spot intensities are confirmed with the exact solutions of the 3D Maxwell equations.

This phenomenon can be used to increase the Raman signal in materials already operating in the breakdown or tunneling regimes and to avoid the modifications of vibrational modes. It can make the SERS imaging of small

Raman-response structures possible. Besides avoiding the heating, it can also be adapted, for instance, for high spatial resolution imaging of molecules. Raman signal emerges from the region where the two plasmon modes overlap spatially. When this overlap area is kept small, better spatial resolution can be obtained. However, SERS process also weakens with reduced overlap integral. The suggested method can compensate this reduction.

Moreover, we provide a clear understanding for the enhancement phenomenon: cancellation (path interference) takes place in the denominator of the SERS response. This understanding makes one raise the following question. Could it be possible to perform better cancellations in the denominator via more sophisticated path interference schemes, by enriching the particle types/numbers generating the interferences?

Acknowledgments: MET acknowledges support from TUBITAK Grant No: 1001-117F118 and TUBA-GEBIP 2017 support.

References

[1] Kauranen M, Zayats AV. Nonlinear plasmonics. Nat Photonics 2012;6:737–8.
[2] Stockman MI. Nanoplasmonics: past, present, and glimpse into future. Opt Express 2011;19:22029–106.
[3] Wu X, Gray SK, Pelton M. Quantum-dot-induced transparency in a nanoscale plasmonic resonator. Opt Express 2010;18: 23633–45.
[4] Höppener C, Lapin ZJ, Bharadwaj P, Novotny L. Self-similar gold-nanoparticle antennas for a cascaded enhancement of the optical field. Phys Rev Lett 2012;109:017402.
[5] He J, Fan C, Ding P, Zhu S, Liang E. Near-field engineering of Fano resonances in a plasmonic assembly for maximizing CARS enhancements. Sci Rep 2016;6:20777.
[6] Hua X, Voronine DV, Ballmann CW, Sinyukov AM, Sokolov AV, Scully MO. Nature of surface-enhanced coherent Raman scattering. Phys Rev A 2014;89:043841.
[7] Wang L-G, Qamar S, Zhu S-Y, Zubairy MS. Manipulation of the Raman process via incoherent pump, tunable intensity, and phase control. Phys Rev A 2008;77:033833.
[8] Chu Y, Banaee MG, Crozier KB. Double-resonance plasmon substrates for surface-enhanced Raman scattering with enhancement at excitation and Stokes frequencies. ACS Nano 2010;4:2804–10.
[9] Luk'yanchuk B, Zheludev NI, Maier SA, et al. The Fano resonance in plasmonic nanostructures and metamaterials. Nat Mater 2010;9:707–15.
[10] Limonov MF, Rybin MV, Poddubny AN, Kivshar YS. Fano resonances in photonics. Nat Photonics 2017;11:543–54.
[11] Nazir A, Panaro S, Zaccaria RP, Liberale C, DeAngelis F, Toma A. Fano coil-type resonance for magnetic hot-spot generation. Nano Lett 2014;14:3166–71.
[12] Tassin P, Zhang L, Koschny T, Economou EN, Soukoulis CM. Low-loss metamaterials based on classical electromagnetically induced transparency. Phys Rev Lett 2009;102:053901.
[13] Liu N, Langguth L, Weiss T, et al. Plasmonic analogue of electromagnetically induced transparency at the Drude damping limit. Nat Mater 2009;8:758–62.
[14] Panaro S, Nazir A, Liberale C, et al. Dark to bright mode conversion on dipolar nanoantennas: asymmetry-breaking approach. ACS Photonics 2014;1:310–4.
[15] Tasgin ME, Salakhutdinov I, Kendziora D, et al. Fluorescence excitation by enhanced plasmon upconversion under continuous wave illumination. Photonic Nanostruct 2016;21:32–43.
[16] Butet J, Bachelier G, Russier-Antoine I, et al. Nonlinear Fano profiles in the optical second-harmonic generation from silver nanoparticles. Phys Rev B 2012;86;075430.
[17] Shorokhov AS, Melik-Gaykazyan EV, Smirnova DA, et al. Multifold enhancement of third-harmonic generation in dielectric nanoparticles driven by magnetic Fano resonances. Nano Lett 2016;16:4857–61.
[18] Singh SK, Abak MK, Tasgin ME. Enhancement of four-wave mixing via interference of multiple plasmonic conversion paths. Phys Rev B 2016;93:035410.
[19] Paspalakis E, Evangelou S, Kosionis SG, Terzis AF. Strongly modified four-wave mixing in a coupled semiconductor quantum dot-metal nanoparticle system. J Appl Phys 2014;115:083106.
[20] Sadeghi SM, Wing WJ, Gutha RR. Undamped ultrafast pulsation of plasmonic fields via coherent exciton-plasmon coupling. Nanotechnology 2015;26:085202.
[21] Emre Ta¸sgın M. Metal nanoparticle plasmons operating within a quantum lifetime. Nanoscale 2013;5:8616–24.
[22] ElKabbash M, Rashed AR, Kucukoz B, et al. Ultrafast transient optical loss dynamics in exciton–plasmon nano-assemblies. Nanoscale 2017;9:6558–66.
[23] Karakul BCY. Enhancement of plasmonic nonlinear conversion and polarization lifetime via Fano resonances, PhD thesis. Middle East Technical University: Ankara, Turkey, 2017.
[24] Noginov MA, Zhu G, Belgrave AM, et al. Demonstration of as paser-based nano laser. Nature 2009;460:1110.
[25] Stockman MI. Nanoscience: dark-hot resonances. Nature 2010;467:541–2.
[26] Zhang Y, Wen F, Zhen Y-R, Nordlander P, Halas NJ. Coherent Fano resonances in a plasmonic nanocluster enhance optical four-wave mixing. Proc Natl Acad Sci 2013;110:9215–9.
[27] Ye J, Wen F, Sobhani H, et al. Plasmonic nanoclusters: near field properties of the Fano resonance interrogated with SERS. Nano Letters 2012;12:1660–7.
[28] Zhang Y, Zhen Y-R, Neumann O, Day JK, Nordlander P, Halas NJ. Coherent anti-Stokes Raman scattering with single-molecule sensitivity using a plasmonic Fano resonance. Nat Commun 2014;5:1–7.
[29] Zhang R, Zhang Y, Dong ZC, et al. Chemical mapping of a single molecule by plasmon-enhanced Raman scattering. Nature 2013;498:82–6.
[30] Kneipp J, Kneipp H, Kneipp K. SERS – a single-molecule and nanoscale tool for bioanalytics. Chem Soc Rev 2008;37: 1052–60.
[31] Qian X, Peng X-H, Ansari DO, et al. In vivo tumor targeting and spectroscopic detection with surface-enhanced Raman nanoparticle tags. Nat Biotechnol 2008;26:83–90.

[32] Yang Y, Callahan JM, Kim T-H, Brown AS, Everitt HO. Ultraviolet nanoplasmonics: a demonstration of surface-enhanced Raman spectroscopy, fluorescence, and photodegradation using gallium nanoparticles. Nano Lett 2013;13:2837–41.
[33] Schaffer CB, Brodeur A, Mazur E. Laser-induced breakdown and damage in bulk transparent materials induced by tightly focused femtosecond laser pulses. Meas Sci Technol 2001;12:1784–94.
[34] Yano T-A, Inouye Y, Kawata S. Nanoscale uniaxial pressure effect of a carbon nanotube bundle on tip-enhanced near-field Raman spectra. Nano Lett 2006;6:1269–73.
[35] Zhu W, Crozier KB. Quantum mechanical limit to plasmonic enhancement as observed by surface-enhanced Raman scattering. Nat Commun 2014;5:5228.
[36] Grosse NB, Heckmann J, Woggon U. Nonlinear plasmon-photon interaction resolved by k-space spectroscopy. Phys Rev Lett 2012;108:136802.
[37] Turkpence D, Akguc GB, Bek A, Tasgin ME. Engineering nonlinear response of nano materials using Fano resonances. J Opt 2014;16:105009.
[38] Mueller NS, Heeg S, Reich S. Surface-enhanced Raman scattering as a higher-order Raman process. Phys Rev A 2016;94:1–13.
[39] Jorio A, Mueller NS, Reich S. Symmetry-derived selection rules for plasmon-enhanced Raman scattering. Phys Rev B 2017;95:1–10.
[40] Finazzi M, Ciccacci F. Plasmon-photon interaction in metal nanoparticles: second-quantization perturbative approach. Phys Rev B 2012;86:035428.
[41] Hohenester U, Trügler A. MNPBEM – a Matlab toolbox for the simulation of plasmonic nanoparticles. Comput Phys Commun 2012;183:370–81.
[42] Tan YH, Liu M, Nolting B, Go JG, Gervay-Hague J, Liu G-Y. A nanoengineering approach for investigation and regulation of protein immobilization. ACS Nano 2008;2:2374–84.
[43] Tasgin ME, Bek A, Postaci S. Fano resonances in optics and microwaves: Physics and Application (Springer Series in Optical Sciences, 2018) Book Chapter 1: Fano resonances in the linear and nonlinear plasmonic response. https://www.springer.com/book/9783319997308. Chapter is available for review purposes: https://www.dropbox.com/s/wkteqhh6rx3tro9/Chapter1.pdf?dl=0.
[44] Brongersma ML, Halas NJ, Nordlander P. Plasmon-induced hot carrier science and technology. Nat Nanotechnol 2015;10:25–34.
[45] Costa SD, Fantini C, Righi A, et al. Resonant Raman spectroscopy on enriched ^{13}C carbonnanotubes. Carbon 2011;49:4719–23.
[46] Scully MO, Zubairy MS. Quantum optics. New York, Cambridge University Press, 1997.
[47] See Supplemental Material for (i) an analytical model for coupling to a long-live dark mode, (ii) for obtaining the SERS Hamiltonian from an optomechanical model, (iii) some details on 3D simulations, and (iv) dependence of the SERS enhancement on the distance of the QE to the hot spot.
[48] Schmidt MK, Esteban R, Gonza´lez-Tudela A, Giedke G, Aizpurua J. Quantum mechanical description of Raman scattering from molecules in plasmonic cavities. ACS Nano 2016;10:6291–8.
[49] Roelli P, Galland C, Piro N, Kippenberg TJ. Molecular cavity optomechanics as a theory of plasmon-enhanced Raman scattering. Nat Nanotechnol 2015;11:164–9.
[50] Premaratne M, Stockman MI. Theory and technology of SPASERs. Adv Opt Photonics 2017;9:79–128.
[51] Garrido Alzar CL, Martinez MAG, Nussenzveig P. Classical analog of electromagnetically induced transparency. Am J Phys 2002;70:37–41.
[52] Min B, Ostby E, Sorger V, et al. High-Q surface-plasmon-polariton whispering-gallery microcavity. Natt Lett 2009;457:455–8.
[53] West PR, Ishii S, Naik GV, Emani NK, Shalaev VM, Boltasseva A. Searching for better plasmonic materials. Laser Photonics Rev 2010;4:795–808.
[54] Liu J-Q, He M-D, Wang D-Y, Tang X-M, Zhang X-J, Zhu Y-Y. Sharp plasmonic resonances based on coupling of high order localized resonance and lattice surface mode in meta-molecules. J Phys D Appl Phys 2013;47:045303.
[55] Huang Y, Zhang X, Ringe E, Hou M, Ma L, Zhang Z. Tunable lattice coupling of multipole plasmon modes and near-field enhancement in closely spaced gold nanorod arrays. Sci Rep 2016;6:23159.
[56] Berthelot J, Bachelier G, Song M, et al. Silencing and enhancement of second-harmonic generation in optical gap antennas. Opt Express 2012;20:10498–508.
[57] "Bem simulations," (sample simulation). Available at: http://physik.uni-graz.at/~uxh/mnpbem/html/mnpbem_ug_bemsimulations.html, accessed: 2017-09–22.
[58] Santhosh K, Bitton O, Chuntonov L, Haran G. Vacuum Rabi splitting in a plasmonic cavity at the single quantum emitter limit. Nat Commun 2016;7:11823.
[59] Hentschel M, Metzger B, Knabe B, Buse K, Giessen H. Linear and nonlinear optical properties of hybrid metallic–dielectric plasmonic nanoantennas. Beilstein J Nanotechnol 2016;7:111–20.
[60] Liu GL, Yin Y, Kunchakarra S, et al. A nanoplasmonic molecular ruler for measuring nuclease activity and DNA footprinting. Nat Nanotech 2006;1:47–52.
[61] Barrow SJ, Wei X, Baldauf JS, Funston AM, Mulvaney P. The surface plasmon modes of self-assembled gold nanocrystals. Nat Commun 2012;3:1275.
[62] Meng L, Huang T, Wang X, Chen S, Yang Z, Ren B. Gold-coated AFM tips for tip-enhanced Raman spectroscopy: theoretical calculation and experimental demonstration. Opt Express 2015;23:13804–13.
[63] Hsiao H-H, Abass A, Fischer J, et al. Enhancement of second-harmonic generation in nonlinear nanolaminate metamaterials by nano photonic resonances. Opt Express 2016;24:9651–9.
[64] Thyagarajan K, Butet J, Martin OJF. Augmenting second harmonic generation using Fano resonances in plasmonic systems. Nano Lett 2013;13:1847–51.

Supplementary Material: The online version of this article offers supplementary material (https://doi.org/10.1515/nanoph-2018-0089).